

1 **Using Eddy Covariance Observations to Determine the Carbon**
2 **Sequestration Characteristics of Subalpine Forests in the Qinghai-**
3 **Tibet Plateau**

4 Niu Zhu^{1,2,4}, Jinniu Wang^{1,2}, Dongliang Luo³, Xufeng Wang³, Cheng Shen^{1,2}, Ning Wu¹

5 1 Chengdu Institute of Biology, Chinese Academy of Sciences, Chengdu 610041,
6 China

7 2 Mangkang Ecological Monitoring Station, Tibet Ecological Security Barrier
8 Ecological Monitoring Network, Qamdo 854500, China

9 3 Northwest Institute of Eco-environmental Resources, Chinese Academy of
10 Sciences, Lanzhou 730000, China

11 4 College of Resources and Environmental Sciences, Gansu Agricultural University,
12 Lanzhou 730070, China

13 **Correspondence:** Jinniu Wang (wangjn@cib.ac.cn)

14 **Abstract:** The subalpine forests are a crucial components in the carbon cycling system in the
 15 Qinghai-Tibet Plateau (QTP). However, there are significant data gaps in the QTP currently, it also
 16 essential to enhance continuous monitoring of forest carbon absorption processes in the future. This
 17 study investigated two years' carbon exchange dynamics of a subalpine forest on the QTP using the
 18 eddy covariance method. We first characterized its seasonal carbon dynamics of the subalpine forest,
 19 revealing the higher carbon dioxide exchange rates in summer and autumn and lower rates in winter
 20 and spring and found that autumn is the peak period for carbon sequestration in the subalpine forest,
 21 with the maximum measured value of CO₂ absorption reaching 10.70 μmol m⁻² s⁻¹. Subsequently,
 22 we explored the environmental factors influencing carbon sequestration function. The PCA analysis
 23 show that photosynthetically active radiation (PAR) was major environmental factor driving the net
 24 ecosystem CO₂ exchange (NEE), significantly influencing forest and carbon absorption, and the
 25 increase of relative humidity decreases the rate of carbon fixation. In addition, we explored NEE
 26 and its influencing factors at the regional scale, found that air temperature promotes carbon dioxide
 27 absorption (negative NEE values), while the average annual precipitation shows a minor effect on
 28 NEE. At the annual scale, the subalpine forest was a strong carbon sink, with an average NEE of
 29 -332~-351 g C m⁻² (from November 2020 to October 2022). Despite facing the challenges of
 30 climate change, forests remain robust carbon sinks with the highest carbon sequestration capacity
 31 in the QTP, with an average annual CO₂ absorption rate of 368 g C m⁻². This study provides valuable
 32 insights into the carbon cycling mechanism in sub-alpine ecosystems and the global carbon balance.

33 **Keywords:** Subalpine forest; Qinghai-Tibet Plateau; The eddy covariance method; Three Parallel
 34 Rivers Region; Carbon sinks

35 **1 Introduction**

36 Carbon dioxide (CO₂) is a prominent greenhouse gas, and its atmospheric concentration has
 37 reached an unprecedented high level in recent years, in May 2021, a recorded peak of 419 parts per
 38 million (ppm) was observed at the Mauna Loa Observatory in Hawaii (Stein, 2021). The global
 39 atmospheric CO₂ concentration is rapidly increasing at a rate of 2 to 3 ppm per year, compared to
 40 pre-industrial levels, the average global temperature has already risen by 1.1 °C by 2019 (World
 41 Meteorological Organization, 2019). Human activities have been the primary catalyst behind the
 42 significant surge in atmospheric CO₂ concentrations (Schweizer et al., 2020). CO₂ and CH₄

- 删除的内容: one of the
- 删除的内容: in the context of climate change and ecosystem dynamics
- 删除的内容: In this study, we
- 删除的内容: the
- 删除的内容: for a subalpine forest on the QTP using the eddy covariance method from November 2020 to October 2022.
- 删除的内容: revealed
- 删除的内容: the
- 删除的内容: characteristics of
- 删除的内容: in
- 删除的内容: revealing the pattern of higher rates in summer and autumn and lower rates in winter and spring.
- 删除的内容: .
- 删除的内容: climatic factors
- 删除的内容: the
- 删除的内容: climatic
- 删除的内容: net ecosystem exchange (NEE)
- 删除的内容: .
- 删除的内容: The spatial distribution of NEE was significantly positively correlated with temperature,
- 删除的内容: at the regional scale
- 删除的内容: of -342 g C m⁻² (from November 2020 to October 2022)
- 删除的内容: caused by climate change, forests remain a robust carbon sink, currently, they are the ecosystems with the highest carbon sequestration capacity in the QTP, with an average annual CO₂ absorption rate of 368 gC m⁻²
- 删除的内容: this
- 删除的内容: essential insights for understanding the carbon cycling mechanism in plateau ecosystems and the global carbon balance.
- 删除的内容: We propose that, to positively influence global carbon cycling, it is essential to enhance continuous monitoring of forest carbon absorption processes in the future.
- 删除的内容: The eddy covariance system
- 删除的内容: .

88 collectively contribute approximately 70% to the global warming potential among the six
89 greenhouse gases specified in the Kyoto Protocol (Zhang et al., 2022). As atmospheric CO₂
90 concentrations continue to rise, global climate warming is gradually intensifying. Therefore, The
91 Paris Agreement urges national governments to restrict the increase in global average temperature
92 to well below 2.0 °C above pre-industrial levels and to strive to limit it to 1.5 °C. The increasing
93 atmospheric CO₂ levels will lead to irreversible ecological disasters. For instance, the concentration
94 of CO₂ in the atmosphere is projected to double within approximately 50 years if global
95 consumption of fossil fuels continues to rise at the current rate. Addressing the greenhouse effect
96 caused by carbon dioxide and reducing its impact is a crucial challenge facing human society today.
97 Reducing regional carbon emissions or per capita carbon emissions is widely regarded as an
98 effective approach to carbon reduction (Wang et al., 2023a). Nevertheless, countries around the
99 world have already begun to commit to carbon reduction and carbon neutrality efforts. On
100 September 22, 2020, during the 75th session of the United Nations General Assembly, the Chinese
101 government announced "double carbon" goals, which aim to achieve carbon emission peaking by
102 2030 and carbon neutrality by 2060, in alignment with ecological conservation and sustainable
103 development objectives (Yu, 2022). It is predicted that China's average forest carbon sequestration
104 rate will reach 0.358 Pg C year⁻¹ by 2060 (Cai et al., 2022). This significant rate of carbon
105 sequestration is expected to have a substantial impact on the environment and economy, providing
106 negative feedback to global warming (Pan et al., 2011).

107 Currently, there are various methods available to accurately quantify the carbon sequestration
108 potential of forests. Quantitative estimation of carbon sequestration potential still requires scientists
109 to establish more *in-situ* sites and generate comprehensive datasets to assess a wide range of areas.
110 Initially, individuals' biomass measurements were used to estimate forest carbon sequestration
111 capacity (Ebermayer, 1876). However, this method was time-consuming, labor-intensive, and prone
112 to inaccuracies due to the omission of various variables during the calculation process. The
113 development of modeling techniques allowed for the use of simulation methods. forest management
114 models and land ecosystem-climate interaction models, such as the Ecological Assimilation of Land
115 and Climate Observation (EALCO), have been widely applied in this regard (Landsberg and Waring,
116 1997; Wang et al., 2001). Currently, remote sensing monitoring and the eddy covariance (EC)

删除的内容: (petagrams of carbon per year)

删除的内容: , each with its advantages and disadvantages

删除的内容: -

120 ~~method~~ are quite popular. Remote sensing techniques can be used to extract vegetation parameters
121 (e.g., ~~normalized difference vegetation index (NDVI)~~) from multispectral bands and estimate the
122 carbon sequestration of entire forests through regression analysis (Laurin et al., 2014). The eddy
123 covariance (EC) method, allowing continuous, long-term carbon flux calculation, provides
124 fundamental data for model establishment and calibration. It ~~has been~~ widely applied across
125 ecosystems, including urban areas, farmlands, grasslands, forests, and water bodies (Konopka et al.,
126 2021; Vote et al., 2015; Du et al., 2022a; Kondo et al., 2017; Li et al., 2022).

127 The forest ecosystem's Net ecosystem exchange (NEE) of carbon dioxide is influenced by
128 multiple environmental factors. Previous studies have shown that NEE is significantly influenced
129 by air temperature (AT), photosynthetically active radiation (PAR), vapor pressure deficit (VPD),
130 relative humidity (RH), and soil temperature (ST) (Liu et al., 2022). For instance, temperature
131 variables, especially annual or seasonal average temperature variations, serve as the optimal single
132 predictor for carbon flux, explaining variations in carbon flux between 19% and 71% (Banbury
133 Morgan et al., 2021). Photosynthetically active radiation not only influences the absorption of
134 carbon dioxide by the forest canopy but also affects the utilization of carbohydrates by roots due to
135 its association with canopy processes and soil respiration (Baumgartner et al., 2020). Furthermore,

136 research suggests that ~~NEE~~ is influenced by biotic factors such as NDVI (Normalized Difference
137 Vegetation Index) and ~~leaf area index (LAI)~~ (Tang et al., 2022). Given the projected future global
138 warming trends, ~~forests play a highly significant~~ vast carbon reservoir ~~for their becoming~~ worthy of
139 attention. The Qinghai-Tibet Plateau (QTP) is the highest and largest plateau in the world, with an
140 extensive area of alpine forests covering approximately 2.3×10^5 km², ~~holding~~ tremendous
141 economic and ecological benefits. The southeastern region of the QTP boasts one of the world's
142 highest-altitude ~~subalpine~~ forest ecosystems. Research indicates that the ~~subalpine~~ forest ecosystem
143 in this area has a remarkable capacity to consume methane, reaching up to 5.06 kg ha⁻¹ yr⁻¹, and
144 playing a significant role in mitigating the impact of greenhouse gases (Qu et al., 2023). ~~Since the~~
145 ~~1960s, the QTP has experienced a faster warming rate than lowland areas, a phenomenon projected~~
146 ~~to intensify by the end of the 21st century~~ (Li et al., 2019). Currently, the QTP is considered a weak
147 carbon sink at the overall level, but the carbon source-sink dynamics vary among different
148 ecosystems (Chen et al., 2022). For instance, most lakes in the QTP are currently characterized by

删除的内容: eddy covariance method

删除的内容: widely used

删除的内容: such as NDVI

删除的内容: is

删除的内容: the

删除的内容: LAI (Leaf Area Index)

删除的内容: the role of

删除的内容: as a

删除的内容: becomes highly significant and

删除的内容: . These forests

删除的内容: Since the 1960s, the QTP has experienced a faster warming rate than lowland areas. It is projected that this phenomenon will be intensified by the end of the 21st century

163 supersaturated CO₂ levels (Cole et al., 1994). Mu et al. (2023) found that the thermokarst lakes serve
 164 as significant carbon sources through carbon flux measurements in 163 thermokarst lakes during
 165 the summer and autumn seasons. Wang et al. (2021) discovered that by comparing carbon fluxes in
 166 ten high-mountain ecosystems with different grassland types, these ecosystems act as sinks for
 167 carbon dioxide. The alpine meadows in the eastern QTP were identified as strong carbon sinks, with
 168 the highest annual average NEE recorded at -284 g C m⁻². Forest ecosystems play a crucial role in
 169 the southeastern edge of the QTP, providing important support for climate regulation and forestry-
 170 based economic activities. Moreover, recent predictive studies suggest that under both current and
 171 future climate scenarios, the forested area in this region is expected to expand further, with
 172 coniferous forests continuing to grow into higher altitudes (Liu et al., 2021). Due to the extensive
 173 presence of permafrost in the QTP, forest net primary productivity exhibits a most pronounced
 174 response to surface temperatures in the continuous permafrost zone over multiple years. Therefore,
 175 the changes in permafrost in the QTP should not be overlooked, as they also have a significant
 176 impact on carbon absorption by forests (Mao et al., 2015). However, the QTP is a vast region with
 177 a widespread distribution of high-altitude and subalpine forests. Long-term monitoring is necessary
 178 to understand how these forests will respond to climate change. Furthermore, there is a significant
 179 data gap concerning the monitoring of carbon exchange capacity in the forests of the QTP,
 180 indicating the need for further data collection efforts. Based on this, we established a carbon flux
 181 monitoring site in the subalpine ecosystem of the Three Parallel Rivers Region, which is located on
 182 the southeastern edge of the QTP and is renowned as a global hotspot for biodiversity (Wang et al.,
 183 2022). Our research objectives are as follows to:

- 184 1) Determine whether the subalpine forests in the Three Parallel Rivers Region act as a carbon
 185 sink or source, and quantify the annual uptake or release of carbon dioxide;
- 186 2) Investigate the influences of main environmental factors influencing the carbon exchange
 187 process in the subalpine forests and identify the factors with the greatest impact, and;
- 188 3) 3) Evaluate the carbon exchange capacity of subalpine forests in the QTP by comparing
 189 existing data with other ecosystems in the region.

190 This study will provide a data foundation and background support for accurately estimating
 191 the carbon balance of forests in high-altitude areas and for model simulations in the future.

删除的内容: discovered that these ecosystems act as sinks for carbon dioxide by comparing carbon fluxes in ten high-mountain ecosystems with different grassland types.

删除的内容: -

删除的内容: Researchers need to conduct long-term monitoring to understand how these forests will respond to climate change.

删除的内容: have

删除的内容: -

删除的内容: lies in the transitional zone between the QTP and the Yunnan-Kweichow Plateau and

删除的内容: Since the carbon sink potential of forest ecosystems in the QTP is currently unknown, we evaluated the carbon exchange capacity of subalpine forests by comparing existing data with other ecosystems in the QTP.

207 **2 Materials and Methods**

208 2.1 Overview of the study site

209 The study site is located in the Hongla Mountain Yunnan Snub-nosed Monkey National Nature

210 Reserve in Mangkang County, Tibet, China (29°17'10.78"N, 98°41'27.45"E), the core area of the
211 watershed of the Three Parallel Rivers (Nujiang River, Lancang River, and Jinsha River) Region.

删除的内容: 29.28633 N, 98.69096 E

删除的内容: the

212 The elevation of the study site is 3755 m. The observation period was from November 2020 to

213 October 2022. The study area experiences large diurnal temperature variations and dry conditions

214 in winter, while the summers are warm and humid. The average daily sunshine duration exceeds 10

215 h, with an annual average temperature of 5 °C and an average annual precipitation of around 600

216 mm within a year (Niu et al., 2023). The main tree species in the area include *Picea likiangensis*

217 *var. rubescens*, *Abies squamata*, *Sabina tibetica* Kom, and *Abies ernestii*. They are accompanied by

218 the growth of some *Quercus aquifolioides*, *Rhododendron lapponicum*, and *Potentilla fruticosa*

219 shrubs. The average height of the trees is around 30 m, and the forest is in a relatively active growth

删除的内容: below

220 phase, reaching the state of a mature forest. The vegetation coverage ranges from 70% to 80%. The

删除的内容: eters

221 dominant soil type is yellow-brown soil. The mountainous terrain contributes to distinct vertical

222 climate characteristics and significant variations in water and heat conditions, with numerous dry

223 and hot river valleys, widespread canyons, and a clear impact from the southwest and southeast

224 monsoons. The varying elevations give rise to diverse ecosystems, transitioning from alpine forests

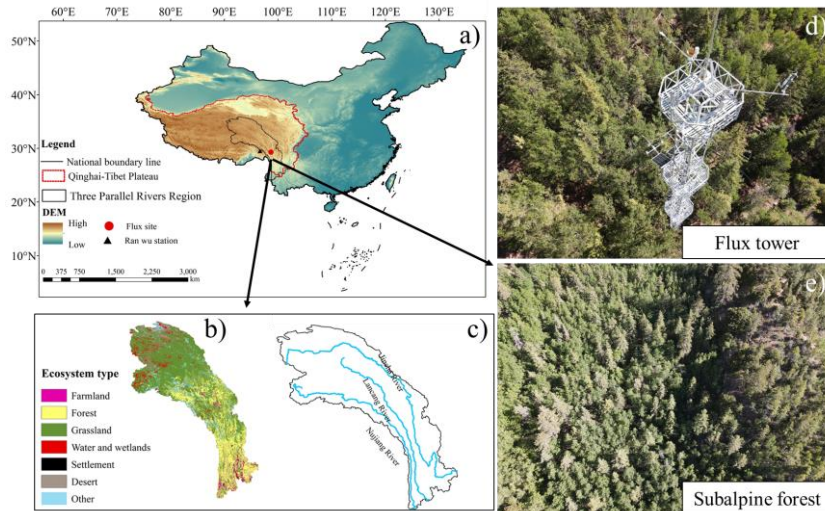
225 to mountain shrubs. Above 4000 m asl, high alpine grasslands and meadows form a noticeable

226 vegetation transition zone. The mountainous topography results in distinct vertical climate features

227 and significant fluctuations in water and heat conditions, with precipitation showing a markedly

228 uneven distribution throughout the study region (Zemin et al., 2023).

删除的内容: The mountainous terrain contributes to distinct vertical climate characteristics and significant variations in water and heat conditions. Characterized by numerous dry and hot river valleys and widespread distribution of canyons, the climate in the study area exhibits a clear impact from the southwest and southeast monsoons. The varying elevations give rise to diverse ecosystems, transitioning from alpine forests to mountain shrubs, and above 4000 meters, high alpine grasslands and meadows, forming a noticeable vegetation transition zone. The mountainous topography results in evident vertical climate features and significant fluctuations in water and heat conditions, with precipitation showing a pronouncedly uneven distribution throughout the region



247
 248 Figure 1. Location of the flux site (a). Ecosystem types (b) and main rivers (c) in the Three Parallel
 249 Rivers Region. Flux tower (d) and forest top view (e). (The national boundary range in the figure
 250 was retrieved from the <http://bzdt.ch.mnr.gov.cn>, and elevation data, and ecosystem type are from
 251 www.gscloud.cn.)

252 2.2 Eddy covariance system

253 The EC system is deployed at a 35 m-high tower, located at the study site. At the top of the
 254 tower, a 3-D wind velocity (Wind Master, Gill, UK) and an open-path infrared CO₂/H₂O analyzer
 255 (LI-7500DS, Li-Cor, USA) were installed to measure CO₂ flux. The instruments had a measurement
 256 frequency of 10 Hz. Additionally, micro-meteorological sensors were placed at different heights on
 257 the tower, including sensors at 35 m for observing air temperature and humidity (HMP155A,
 258 Vaisala, Finland), sensors at -5 cm for soil temperature (TEROS11, LI-Cor, USA), and sensors at
 259 35 m for photosynthetically active radiation (LI-190R, LI-Cor, USA). All data was stored for 30-
 260 minute in a SmartFlux 3 data logger (Li-Cor, USA) for future download.

261 2.3 Data processing and quality control

262 When considering only the turbulent transport of matter and energy in the vertical direction,
 263 the carbon dioxide flux (F_c) can be represented by the following equation (Yu and Sun, 2006;
 264 Monteith et al., 1994):

265
$$F_c = \overline{W'CO_2'} \quad (1)$$

删除的内容: location

删除的内容: The flux data in this study were collected from a 35 m-high tower

删除的内容: , among other environmental variables

删除的内容: All data were recorded at 30-m intervals and stored in

272 Where W' is the vertical component of 3-D wind speed fluctuations (m s^{-1}), and CO_2' represents the
273 fluctuations in measured CO_2 mole concentration. A positive F_c indicates carbon emissions, while
274 a negative value represents carbon uptake.

275 The acquired 10 Hz raw data was processed and corrected using the EddyPro software
276 (EddyPro 7.06, Li-Cor, USA). The calibration process involved outlier detection for flux data, lag
277 elimination, coordinate rotation (Jia et al., 2020), ultrasonic temperature correction (Schotanus et
278 al., 1983), frequency correction (Moncrieff et al., 1997), and Webb-Pearman-Leuning (WPL)
279 correction (Leuning and King, 1992). After these controls, the integrity of the effective FC raw ~~data~~
280 valid data we obtained reached 92.95 %. We removed outliers caused by environmental disturbances
281 such as power outages, rain, snow, and dust particles that interfered with the instrument. Due to the
282 slope of the underlying surface being around 5 degrees, we also corrected from non-uniform and
283 non-flat surfaces using EddyPro for ~~double~~-coordinate rotation (Cao et al., 2019). As a result, we
284 obtained half-hourly flux data with associated data quality indicators. To evaluate the turbulence
285 steadiness, we employed the "0-1-2" quality assessment method, which classified flux results into
286 three quality levels: 0 for excellent data quality, 1 for moderate data quality, and 2 for low data
287 quality (Mauder and Foken, 2011; Foken et al., 2005). We removed data points labeled with a quality
288 level of "2". We further eliminated flux data with negative values during nighttime since plants do
289 not perform photosynthesis at night. Additionally, we conducted spectral analysis to identify and
290 remove data points with values significantly deviating from normal. Finally, friction velocities (u^*)
291 for each of the two years were determined separately using the method of moving point, and deleted
292 data recorded during nighttime when u^* was less than 0.28 and 0.39 m s^{-1} (Reichstein et al., 2005).
293 After excluding outliers from the data, the data integrity is 72.67%. Tovi software (Tovi, Li-Cor,
294 USA) was used in the process.

295 When turbulence is weak, a portion of CO_2 is stored in the vegetation canopy and the
296 atmosphere below the measurement height. At this time, the NEE is calculated as (Zhang et al.,
297 2018):

$$298 \quad \text{NEE} = F_c + F_s \quad (2)$$

299 Where NEE represents the net ecosystem exchange of CO_2 , F_c stands for the observed flux during
300 a specific period, F_s represents the CO_2 storage in the forest canopy, F_s is calculated as $(\Delta c/\Delta t) \cdot h$,

删除的内容:),

删除的内容: double

303 where Δc is the difference in CO_2 concentration between two consecutive measurements, Δt is the
304 time interval between two consecutive measurements, and h is 35m.

305 We adopted the following formula as a gap-filling strategy for daytime NEE (NEE_{day})
306 concerning PAR, aiming to address missing values during the daytime (Falge et al., 2001):

307
$$\text{NEE}_{\text{day}} = \frac{\alpha \cdot \text{PAR} \cdot P_{\text{max}}}{\alpha \cdot \text{PAR} + P_{\text{max}}} - R_{\text{day}} \quad (3)$$

308 where, α ($\mu\text{mol CO}_2/\mu\text{mol PAR}$) represents the apparent photosynthetic quantum efficiency, which
309 characterizes the maximum efficiency of converting light energy during photosynthesis; PAR (μmol
310 $\text{m}^{-2} \text{s}^{-1}$) is the photosynthetically active radiation, a measure of the amount of light energy available
311 for photosynthesis; P_{max} ($\mu\text{mol CO}_2 \text{ m}^{-2} \text{ s}^{-1}$) is the apparent maximum photosynthetic rate,
312 representing the maximum CO_2 uptake rate under optimal conditions, and; R_{day} ($\mu\text{mol CO}_2 \text{ m}^{-2} \text{ s}^{-1}$)
313 is the daytime dark respiration rate, which denotes the rate of CO_2 release during daylight hours.
314 The parameters α , P_{max} , and R_{day} are obtained through the non-linear fitting of the Michaelis-Menten
315 model to the observed data.

316 During the nighttime, the NEE is modeled using an exponential function of ecosystem
317 respiration and soil temperature to fill in the missing values of NEE during the night ($\text{NEE}_{\text{night}}$)
318 (Lloyd and Taylor, 1994; Kato et al., 2006):

319
$$\text{NEE}_{\text{night}} = a \cdot \exp^{(bt)} \quad (4)$$

320 Where a and b are estimated values for the exponential function used in modeling $\text{NEE}_{\text{night}}$, and; The
321 variable t represents the soil temperature measured at the depth of 5 cm. Origin 2023 (Originlab
322 Corporation, USA) is the data processing software used for this analysis. For the missing data,
323 interpolation was performed using Tovi software allows for data interpolation to fill in the gaps and
324 ensure a continuous dataset for further analysis (Reichstein et al., 2005). **27.33% of missing data**
325 **were interpolated using Tovi after filtering, resulting in a flux data set with complete data integrity.**

326 In flux analysis, the significance of source area contributions cannot be overlooked. In this
327 study, the peak distances of the 90% flux contribution areas averaged over two years are 364.2 and
328 357.1m, In terms of seasons, the average peak distances of the 90% flux contribution areas for winter,
329 spring, summer, and autumn over the two years are as follows: 353.9, 358.2, 350.05, and 344.34m,
330 respectively.

删除的内容: .

删除的内容: .

删除的内容: .

删除的内容: .

带格式的: 字体颜色: 红色

删除的内容: The parameters

删除的内容: .

删除的内容: 27.33% of missing data were interpolated, The final flux data achieved a data integrity of 100%.

删除的内容: respectively. Looking at seasons, the average peak distances of the 90% flux contribution areas for winter, spring, summer, and autumn over the two years are 353.9, 358.2, 350.05, and 344.34m, respectively.

343 2.4 Flux partitioning

344 Ecosystem respiration (RE) is the sum of plant and heterotrophic respiration in an ecosystem
345 and is obtained by adding the measured nighttime data to the extrapolated daytime data. Gross
346 primary productivity (GPP) is the total amount of organic carbon fixed by green plants through
347 photosynthesis per unit of time and per unit of area:

348
$$RE=R_{\text{day}}+R_{\text{night}} \quad (5)$$

349
$$GPP=-NEE+RE \quad (6)$$

350 Carbon use efficiency (CUE) is a crucial parameter that reflects the ability of an ecosystem to
351 sequester carbon. It is defined as the ratio of net ecosystem productivity (NEP) to gross primary
352 productivity. CUE can be expressed using the following equation:

353
$$CUE=\frac{NEP}{GPP}=\frac{-NEE}{GPP} \quad (7)$$

354 To study the variation of ecosystem respiration rates with environmental factors, we considered
355 the dependence of nocturnal ecosystem respiration on soil temperature (Pavelka et al., 2007;
356 Mamkin et al., 2023):

357
$$Q_{10}=\exp(10 \cdot \alpha) \quad (8)$$

358
$$\ln(NEE_{\text{night}})=\alpha \cdot T+\gamma \quad (9)$$

359 Where T is the soil temperature (°C) and γ is an empirical parameter of the equation.

360 To clarify the carbon sink potential of forests in the QTP and to compare it with other
361 ecosystems, a search was conducted in two authoritative databases, Web of Science and China
362 National Knowledge Internet, for research articles on the current utilization of EC systems in the
363 QTP. A total of 82 research results were collected from 48 studies, and their annual average
364 environmental factors, such as air temperature, precipitation, and altitude, were obtained.

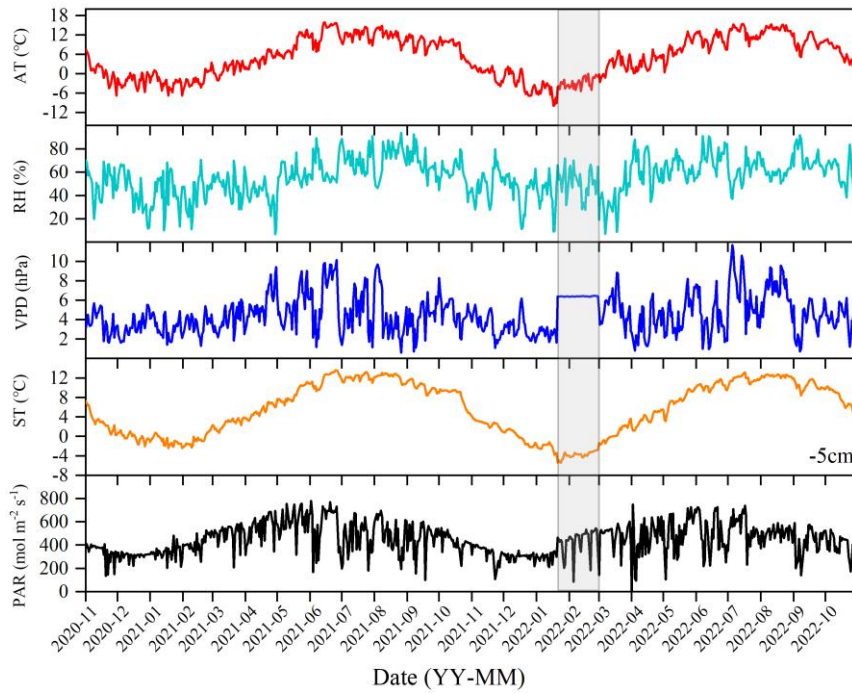
365 **3 Results**

366 **3.1 Daily changes in main environmental factors**

367 During the observational period, the environmental conditions exhibited significant
368 fluctuations. The winter and spring seasons were characterized by cold and dry conditions, while
369 the summer and autumn seasons were warm and humid. The daily maximum A_T recorded was
370 15.87 °C (on June 15, 2021), and the minimum temperature was -9.88 °C (on January 17, 2022),
371 with a mean annual average of 5.5 °C over the two years. RH is average at 55.89% and VPD is

- 删除的内容: average
- 删除的内容: air temperature (
- 删除的内容:)
- 删除的内容: n
- 删除的内容: The relative humidity (
- 删除的内容:)
- 删除的内容: with an annual
- 删除的内容: of
- 删除的内容: . The
- 删除的内容: vapor pressure deficit (
- 删除的内容:)
- 删除的内容: with an

384 annual average d at 4.46 hPa. ST exhibited a similar trend to air temperature. The highest observed
 385 soil temperature was 13.53 °C (on June 27, 2021), while the minimum was -3.78 °C (on January 18,
 386 2022), with an annual average of 6.11 °C. PAR is averaged at 447.24 mol m⁻² s⁻¹.



387
 388 Figure 2. Daily values of main environmental factors, air temperature (AT), relative humidity (RH),
 389 vapor pressure deficit (VPD), soil temperature (ST), and photosynthetically active radiation (PAR).
 390 (The data of the shadow part in the figure comes from the Ranwu forest site (Figure 1). Since there
 391 was no interpolated data source for VPD, the annual average was used instead.)

392 **3.2 Seasonal dynamics of NEE, RE, and GPP**

393 The observations from the forest ecosystem indicate distinct diurnal and seasonal variations in
 394 NEE and GPP (Figure 3). The NEE and GPP exhibit a pronounced U-shaped curve, with significant
 395 seasonal differences. The summer and autumn are characterized by peak carbon uptake, with the
 396 maximum NEE reaching. During the nighttime, the ecosystem generally releases carbon, while
 397 during favorable daytime meteorological conditions, it demonstrates a carbon uptake capacity. The
 398 peak carbon absorption of the forest ecosystem occurs from 12:00 to 15:00 (Beijing time,
 399 UTC+8:00). The daily carbon sequestration in summer and autumn is 1.5-3 hrs longer than in winter.

删除的内容: of
 删除的内容: Soil temperature (
 删除的内容:)
 删除的内容: Photosynthetically active radiation (
 删除的内容:)
 删除的内容: with an annual average of

删除的内容: Photosynthetically

删除的内容: The s

408 The timing of maximum carbon sequestration capacity changes with each season. In winter, the
 409 transition from nighttime carbon release to daytime carbon uptake occurs around 08:30, which is
 410 approximately 1 hour later than in summer. GPP characterizes the forest's carbon sequestration
 411 capacity, and since photosynthesis does not occur at night, GPP is zero during nighttime. The
 412 maximum daily total productivity is recorded at $14.76 \pm 7.34 \mu\text{mol CO}_2 \text{ m}^{-2} \text{ s}^{-1}$ during the summer
 413 of the second year, with a standard deviation indicating greater variability in GPP and NEE during
 414 the summer and autumn compared to the winter and spring. Although diurnal variations in RE are
 415 relatively small, there are significant seasonal differences. During the night, when only respiration
 416 occurs, RE equals NEE. However, as photosynthesis becomes active during the day, RE gradually
 417 increases and stabilizes. The respiratory rate of the coniferous forest is highest in autumn, being
 418 eight times greater than in winter.

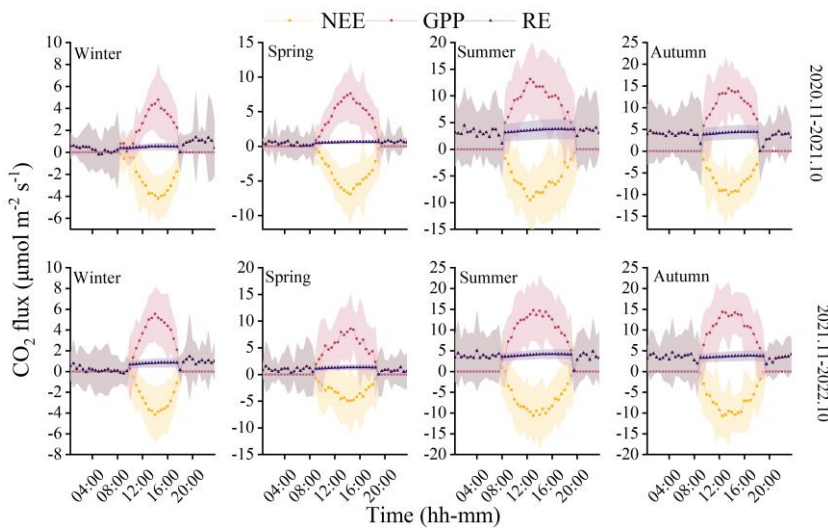


Figure 3. Monthly mean values of CO₂ fluxes.

删除的内容: carbon fluxes

419

420

421 3.3 Relationship between NEE and main environmental factors

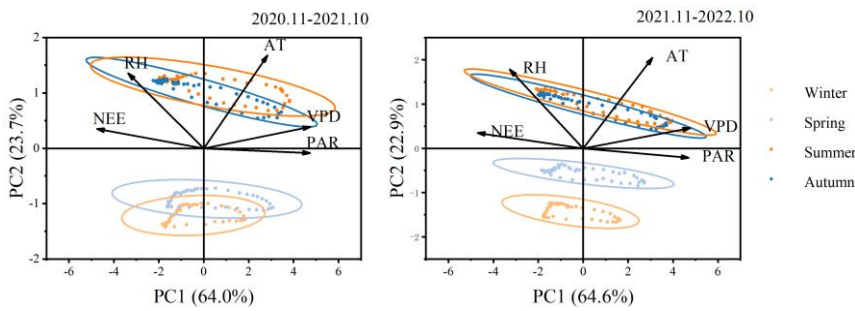
422

The PCA analysis of NEE and environmental factors (Figure 4) indicates that the explanations
 423 for the first principal component (PC1) and the second principal component (PC2) are essentially
 424 the same between the two years. The total contributions of PC1 and PC2 are 87.7% and 87.5%,
 425 respectively, with PC1 accounting for 64.0% and 64.6% individually. The angle between
 426 photosynthetically active radiation (PAR) and PC1 is minimal, suggesting a strong correlation

删除的内容: two years of

429 between PAR and PC1. Additionally, PAR and VPD contribute the most to PC1, while AT and RH
 430 contribute the most to PC2. The analysis results reveal a significant positive correlation between
 431 NEE and RH, while a significant negative correlation is observed with AT, VPD, and PAR.
 432 Increased RH is detrimental to forest carbon dioxide absorption. Excessively high relative humidity
 433 causes plant leaf stomata to close, reducing the amount of carbon dioxide available to the plant. This,
 434 in turn, leads to a decrease in the efficiency of carbon fixation through photosynthesis. Among these
 435 environmental factors, PAR plays a dominant role. Furthermore, the figure illustrates the
 436 relationships between environmental factors, showing a positive correlation between RH and TA,
 437 and a negative correlation with VPD and APR. The indicators exhibit some seasonality, with notable
 438 differences between the winter-spring and summer-autumn seasons, indicating limited similarity
 439 between seasons.

删除的内容: This implies that an increase in RH is unfavorable for the forest's absorption of carbon dioxide.



440
 441 Figure 4. Principal component analysis of environmental factors and NEE

442 3.4 Seasonal variation of NEE, GPP, and RE

删除的内容: characteristics

443 The NEE did not show significant inter-seasonal differences (Figure 5). However, data
 444 distribution indicates that the variability in NEE rate differs across different seasons, particularly
 445 between summer-autumn and winter-spring. The changes in GPP over the two years were similar,
 446 with significant differences observed between summer and winter ($P < 0.05$). The RE was higher
 447 during summer-autumn compared to winter-spring. The highest ecosystem respiration occurred in
 448 the first year during autumn, while in the second year, it was highest during summer. Within the
 449 same year, summer and autumn exhibited significant differences ($P < 0.05$), while between the same
 450 seasons in different years, notable distinctions were not observed. This pattern is also reflected in
 451 GPP and NEE.

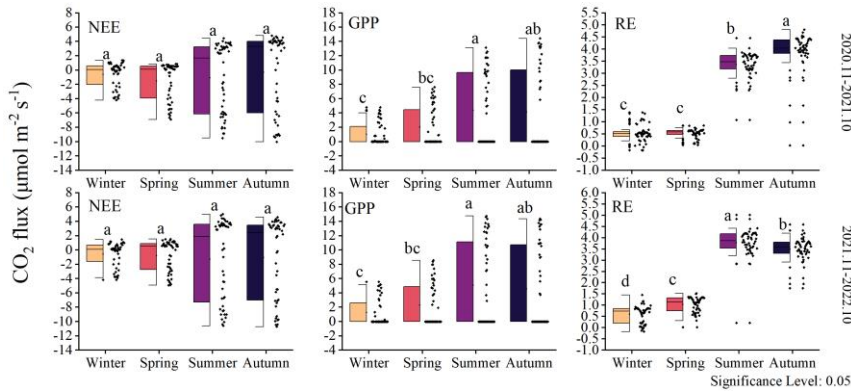


Figure 5. Seasonal variation of CO₂ fluxes in two years.

删除的内容: carbon fluxes

3.5 Changes in total NEE, GPP, RE, and CUE

The cumulative fluxes over the two years for the forest ecosystem are shown in Figure 6. NEE indicates the net carbon sequestration in each month. The cumulative respiration reached its highest value of 361 g C m⁻² in the summer of 2022. The total NEE, GPP, and RE for the first year were -332, 1121, and 788 g C m⁻², respectively, and -351, 1199, and 847 g C m⁻² for the second year, respectively. The CUE was higher during the spring and lower during the autumn, with a maximum value of 0.74 and a minimum value of 0.07. The average CUE over the two years was 0.40 and 0.35, respectively.

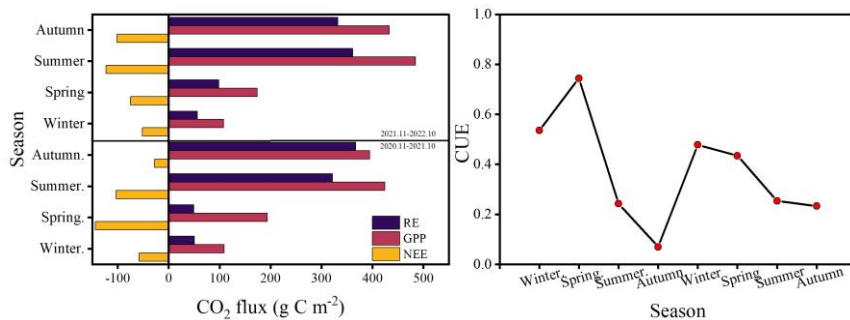
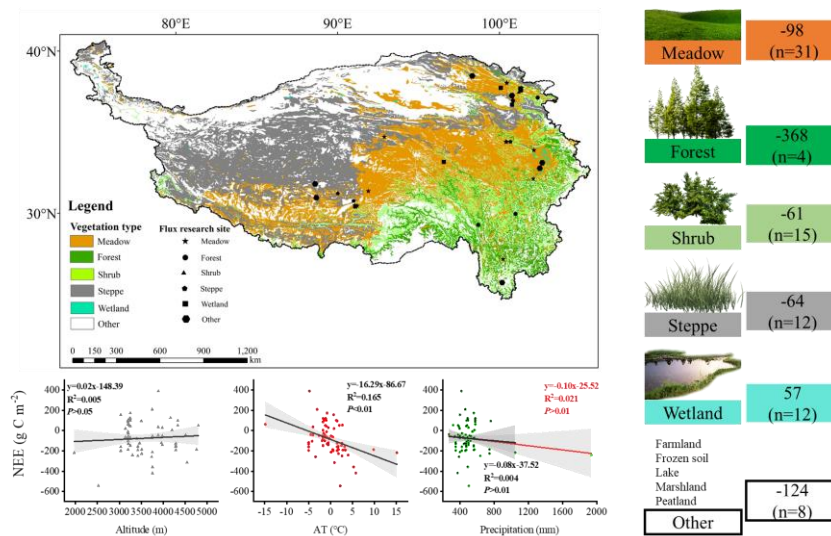


Figure 6. Change in total carbon flux and carbon use efficiency

3.6 The carbon sequestration potential of subalpine forests of QTP

To clarify the carbon sequestration contribution of the subalpine forests found in the QTP, we compared these research results (Figure 7). Found that ecosystems with high vegetation cover

471 exhibited higher annual cumulative carbon sequestration. Among these ecosystems, the subalpine
 472 forests in the QTP showed the highest carbon sequestration potential, reaching an average of 368 g
 473 C m⁻² per year. The carbon sequestration potential of different ecosystems ranked as follows: forest >
 474 meadow > steppe > shrub. The average value for wetlands indicated that they are a significant source
 475 of CO₂, releasing 57 g C m⁻² into the atmosphere annually. We also analyzed the influence of altitude,
 476 mean annual air temperature, and precipitation on NEE at these sites in the QTP. It has been
 477 observed that these sites cover a wide range of altitudes, ranging from 1977 to 4800 m. According
 478 to existing results, an increase in elevation may lead to a reduction in carbon uptake, while the range
 479 of mean annual temperature varies between -14.8 to 15.1 °C, and higher mean annual temperatures
 480 significantly increase carbon uptake. Forests exhibit the highest mean annual precipitation,
 481 averaging 827 mm, with mean annual precipitation having a relatively weak impact on the NEE.
 482 These findings highlight the important role of subalpine forests in carbon sequestration in the QTP
 483 and provide insights into the factors that affect carbon exchange in the QTP, such as altitude,
 484 temperature, and precipitation.



485
 486 Figure 7. Carbon exchange potential of different ecosystems in the Qinghai-Tibet Plateau

487 **4 Discussion**

488 **4.1 Main factors affecting the carbon sequestration function of subalpine forests**

489 Climate change significantly affects the vegetation's carbon sequestration capacity, particularly
490 at the seasonal scale due to phenological changes (Acosta-Hernández et al., 2020). In the short term,
491 PAR, AT, RH, and VPD play important roles in regulating vegetation photosynthesis and,
492 consequently, carbon uptake. For instance, PAR represents the portion of solar energy that can be
493 utilized by plants and is an essential component in chloroplast reactions. PAR drives a nonlinear
494 response of GPP to Solar-induced fluorescence (SIF) across different seasons, resulting in a strong
495 positive correlation between GPP and SIF (Wang et al., 2023b). VPD affects photosynthesis and
496 transpiration of leaves, with stomata serving as tiny pores mediating carbon dioxide uptake.
497 Research has demonstrated that excessive increases in VPD are detrimental to photosynthesis. For
498 instance, a moderate increase in VPD significantly reduces photosynthetic efficiency under light
499 fluctuations due to changes in RH and/or AT often accompanying fluctuations in light, studies also
500 indicate that the impact of VPD on sunlight utilization efficiency is primarily determined by relative
501 RH rather than AT (Liu et al., 2024). In different seasons, the same influencing factors exhibit
502 varying degrees of contribution to NEE. For example, during winter, when the climatic conditions
503 are relatively harsh with low air temperature and humidity, the forest maintains a low level of carbon
504 uptake. On longer time scales, such as annual and decadal variations, the inherent changes in forest
505 NEE may be attributed to disturbances and recovery (Hayek et al., 2018). In this study, significant
506 differences in ecosystem respiration were observed during the summer and autumn in different years.
507 Previous studies suggested that due to leaf aging or water stress, the photosynthetic light use
508 efficiency of the ecosystem peaks after spring leaf expansion and gradually declines (Wehr et al.,
509 2016). This implies a peak in carbon exchange during the summer, followed by higher productivity
510 and ecosystem respiration in the following seasons. The variation in different years may be
511 attributed to rainfall regulating the availability of natural resources such as water, biomass, litter,
512 and soil nutrients (Schwinning and Sala, 2004). For instance, in temperate forests, when microbial
513 biomass undergoes seasonal changes, microbial activity exhibits a seasonal lag in response to
514 temperature variation, resulting in a seasonally delayed effect between litter heterotrophic
515 respiration and temperature (Ataka et al., 2020). Whether such differences persist between different
516 years on longer time scales remains to be demonstrated through more sustained and detailed
517 research in the future. Ecosystem respiration sensitivity to temperature is represented by the Q_{10}

删除的内容: these factors (

删除的内容:)

删除的内容: representing

删除的内容: ,

删除的内容: accompany

删除的内容: 。

删除的内容: Past research

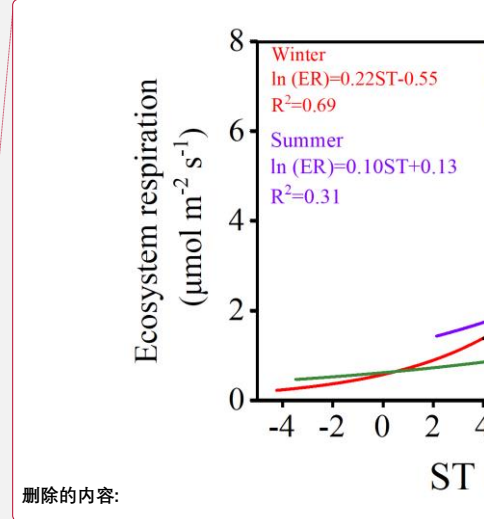
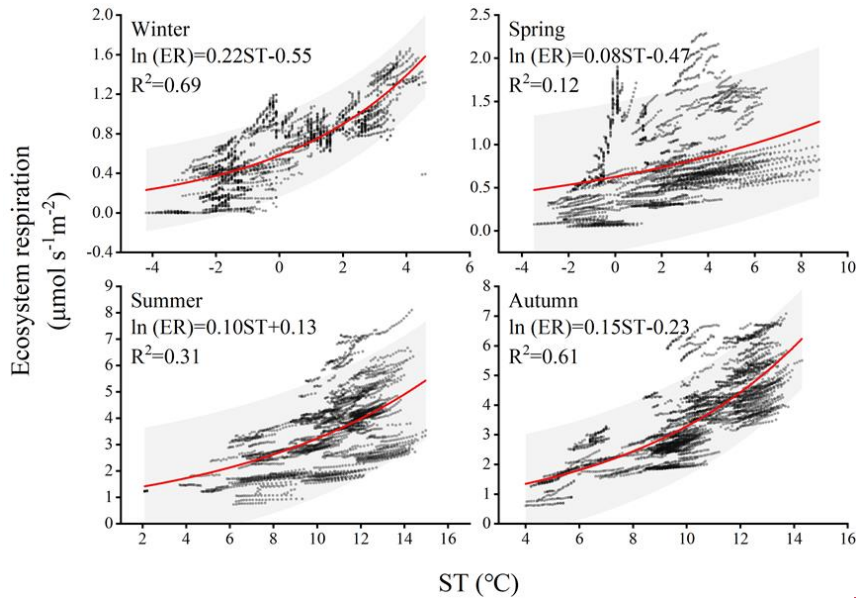
525 coefficient. In this study, seasonal variations influenced the magnitude of Q_{10} (as shown in Figure
526 8). The calculated Q_{10} for each season are as follows: ~~9.03, 2.22, 2.71, and 4.48~~. The winter season
527 exhibited the highest sensitivity of forest ecosystem respiration to temperature, indicating that
528 respiration rates in the winter are more responsive to changes in temperature compared to other
529 seasons. The main reason for such differences is that ecosystem respiration consists of heterotrophic
530 respiration and autotrophic respiration, which are typically governed by different factors (Edwards,
531 1975). For instance, the high activity of soil microbes contributes to heterotrophic respiration, a
532 process dominated by soil temperature and moisture conditions, which are severely restricted during
533 the cold and dry conditions of winter (Falge et al., 2002). Simultaneously, due to the changing
534 relative roles of growth and maintenance respiration, the allocation of autotrophic respiration varies
535 seasonally. In winter, soil CO_2 emissions constitute a significant portion of ecosystem CO_2
536 emissions, and in some boreal forests, the ratio between the two can reach 0.6 or even higher
537 (Davidson et al., 2006). In winter, under the frequent coverage of snow, cold-adapted
538 microorganisms thriving in a relatively narrow sub-zero temperature range engage in respiration
539 and exhibit relatively high sensitivity to warming or cooling beyond this range (Monson et al., 2006).
540 The seasonal patterns of the Q_{10} value are jointly determined by the variation in the ratio of soil
541 respiration to ecosystem respiration, reflecting these seasonal changes.

删除的内容: 9.025, 2.22, 2.71, and 4.48.

542 Our integrated analysis (as shown in Figure 7) reveals that despite the high elevation of the
543 "Third Pole", the topographic factor of elevation does not have a significant impact on carbon uptake.
544 Instead, NEE gradually increases with a steep rise in elevation. Research conducted by Wang et al.
545 (2023c) ~~has indicated that~~ mean annual average temperature and precipitation are the main driving
546 factors of interannual variations in NEE in alpine meadows and alpine steppes. Decreased
547 precipitation ~~resulted~~ in a transition into carbon sources at some regions with high precipitation-
548 dependent alpine grasslands. It is worth noting that, among all data collection sites, alpine wetlands
549 show an average carbon source trend. Due to prolonged flooding and low temperatures, microbial
550 activity in alpine wetlands is hindered, and the accumulation of organic carbon from plant litter
551 decomposition is substantial. As a result, approximately 57 g C m^{-2} is emitted into the atmosphere
552 annually. Previous studies have indicated that NEE in alpine wetlands is increasing with global
553 warming (Yasin et al., 2022).

删除的内容: indicates that

删除的内容: resulting



删除的内容:

删除的内容: absorbing

删除的内容: .

删除的内容: serve

557

558 Figure 8. Relationship between NEE_{night} and soil temperature in different seasons

559 4.2 Sustained carbon sequestration of subalpine forests

560 Subalpine forests are integral components of global alpine ecosystems and play crucial roles
 561 in the global carbon cycle. Our study on subalpine forests demonstrates a continuous absorption of
 562 carbon dioxide even during winter, which aligns well with measurements taken in the vicinity of
 563 Mount Fuji in Japan (Mizoguchi et al., 2012). The age of subalpine forests is a crucial factor
 564 influencing sustained carbon sequestration. Based on NPP simulations of natural subalpine forests
 565 in the Northern Rockies, Carey (2001) found that aboveground net primary productivity reaches its
 566 maximum after approximately 250 years, followed by a decline, this challenges the previous view
 567 that forests older than 100 years are generally considered to be unimportant carbon sinks. Compared
 568 to the forest (mature forest) of Mount Gongga in the QTP (e.g., Zhang et al., 2018), the subalpine
 569 forest in this study exhibits a stronger carbon sequestration capacity. However, its carbon
 570 sequestration ability is slightly weaker than that of the Qilian Mountains high-mountain forests
 571 (approximately 60-70 years old) in the QTP (Zhang et al., 2018; Du et al., 2022b). Although existing
 572 flux monitoring results of high-altitude forests in the QTP indicate that these forest ecosystems act
 573 as carbon sinks, it is important to consider that globally there are still many cold regions with
 574 coniferous forests servig as carbon sources. For example, continuous CO₂ flux monitoring from

579 native boreal forests in Sweden for over 10 years indicates that they are a net carbon source, which
580 is attributed to the contribution of woody debris to RE due to disturbances such as extreme weather
581 events, fires, insect infestations, and pathogen attacks (Hadden and Grelle, 2017). In the summer of
582 2018, Europe experienced a heatwave that affected the carbon cycling in forests. The mixed
583 coniferous-deciduous forest in southern Estonian, under the influence of the heatwave, transitioned
584 from a net carbon sink to a net carbon source in 2018 (Krasnova et al., 2022). Particular attention
585 should be paid to the long-term monitoring in high-altitude environments of the impact of
586 disturbances on forest carbon sequestration capacity. Our study has shown that forests in the QTP
587 have the strongest carbon sink capacity, indicating that alpine forests will have an important
588 sustained effect on carbon reduction in the QTP in the context of future climate change, but whether
589 this sustained effect will be longer than other ecosystems is still unknown. However, a modeling
590 experiment in a large semi-arid area of California predicted that grasslands are more resilient carbon
591 sinks than forests in responding to climate change in the 21st century (Dass et al., 2018). In terms
592 of carbon sequestration rate, forests in the QTP were significantly stronger than other ecosystems,
593 followed by grasslands, while alpine deserts and alpine grasslands in the north-western and southern
594 regions were the main carbon sources (Wu et al., 2022). Forests are mostly distributed in the south-
595 eastern margin of the QTP and the mid-altitude area near 3000 m in the Sichuan-Tibet alpine gorge
596 area, with an area of $19.3 \times 10^4 \text{ km}^2$ (Yu et al., 2022). Based on the average value of a few current
597 carbon flux monitoring, the forest in the QTP will absorb about $71 \times 10^6 \text{ Mg C year}^{-1}$.

598 **5 Conclusion**

599 This study explores the carbon sequestration function, seasonal variations, and climate drivers
600 of subalpine forests in the QTP. Over the observational period, we synchronously monitored
601 ecosystem carbon exchange and primary environmental factors using an eddy covariance system.

602 The research reveals that the subalpine forest acts as a carbon sink. Over the two years, the total
603 NEE, GPP, and RE were $-332, 1121, \text{ and } 788 \text{ g C m}^{-2}$ in first year, and $-351, 1199, \text{ and } 847 \text{ g C m}^{-2}$
604 in second year. Photosynthetically active radiation was identified as the primary control of NEE.
605 Relative humidity is negatively correlated with NEE, and its increase is not conducive to carbon
606 sink. NEE reached its peak in autumn. Combining results from other eddy covariance sites on the
607 QTP, this study highlights that forests have the highest carbon sequestration potential, reaching 368

删除的内容: We

删除的内容: The research reveals that the subalpine forest is a carbon sink, with a total NEE, GPP, and RE of $-332, 1121, \text{ and } 788 \text{ g C m}^{-2}$, respectively, and $-351, 1199, \text{ and } 847 \text{ g C m}^{-2}$ for two years, respectively.

删除的内容: .

614 ~~g C m⁻² annually, followed by meadows (-98 g C m⁻²), steppes (-64 g C m⁻²), and shrubs (-61 g C~~
615 ~~m⁻²). In contrast, wetlands were identified as a significant source of carbon dioxide (57 g C m⁻²).~~

616 Despite the challenges posed by climate change, the subalpine forests in the QTP retain substantial
617 carbon sequestration potential. Strengthening conservation and management efforts for subalpine
618 forests is crucial to ensure their continued and significant carbon sequestration function in the future.
619 Overall, this research underscores the vital role of subalpine forests in the QTP as essential carbon
620 sink regions, playing a critical role in the context of global climate change.

621 **Data availability.** The data is available from the authors on request.

622 **Authorship contributions.** **Niu Zhu:** Conceptualization, study design, data analyses,
623 visualization, writing—original draft. **JinNiu Wang:** study design, writing—review & editing,
624 supervision, project administration, funding acquisition. **Dongliang Luo and Xufeng Wang:**
625 writing—reviewing & editing. **Cheng Shen and Ning Wu:** resources, data curation, supervision. all
626 authors approved the final manuscript.

627 **Declaration of competing interest.** The authors declare that they have no conflict of interest.

628 **Acknowledgements.** We thank Ms. Neha Bisht for her substantial comments and language
629 revision to improve the manuscript. This study was funded by CAS "Light of West China" Program
630 (2021XBZG-XBQNXZ-A-007); The National Natural Science Foundation of China (31971436);
631 The State Key Laboratory of Cryospheric Science, Northwest Institute of Eco-Environment and
632 Resources, Chinese Academy Sciences (SKLCS-OP-2021-06).

633 Reference

634 Acosta-Hernández, A. C., Padilla-Martínez, J. R., Hernández-Díaz, J. C., Prieto-Ruiz, J. A., Goche-Telles,
635 J. R., Nájera-Luna, J. A., and Pompa-García, M.: Influence of Climate on Carbon Sequestration in
636 Conifers Growing under Contrasting Hydro-Climatic Conditions, *Forests*, 11, 1134, 2020.

637 Ataka, M., Kominami, Y., Sato, K., and Yoshimura, K.: Microbial Biomass Drives Seasonal Hysteresis
638 in Litter Heterotrophic Respiration in Relation to Temperature in a Warm-Temperate Forest, *Journal of*
639 *Geophysical Research: Biogeosciences*, 125, e2020JG005729, <https://doi.org/10.1029/2020JG005729>,
640 2020.

641 Banbury Morgan, R., Herrmann, V., Kunert, N., Bond-Lamberty, B., Muller-Landau, H. C., and
642 Anderson-Teixeira, K. J.: Global patterns of forest autotrophic carbon fluxes, *Global Change Biology*,

删除的内容: The NEE did not exhibit significant differences across seasons. Combining results from other eddy covariance sites on the QTP, this study highlights those forests have the highest carbon sequestration potential, reaching 368 g C m⁻² annually, followed by meadows, steppes, and shrubs. Wetlands, however, were identified as a substantial carbon dioxide source

650 27, 2840-2855, <https://doi.org/10.1111/gcb.15574>, 2021.

651 Baumgartner, S., Barthel, M., Drake, T. W., Bauters, M., Makelele, I. A., Mugula, J. K., Summerauer, L.,
652 Gallarotti, N., Cizungu Ntaboba, L., Van Oost, K., Boeckx, P., Doetterl, S., Werner, R. A., and Six, J.:
653 Seasonality, drivers, and isotopic composition of soil CO₂ fluxes from tropical forests of the Congo Basin,
654 *Biogeosciences*, 17, 6207-6218, [10.5194/bg-17-6207-2020](https://doi.org/10.5194/bg-17-6207-2020), 2020.

655 Cai, W., He, N., Li, M., Xu, L., Wang, L., Zhu, J., Zeng, N., Yan, P., Si, G., and Zhang, X.: Carbon
656 sequestration of Chinese forests from 2010 to 2060: Spatiotemporal dynamics and its regulatory
657 strategies, *Science Bulletin*, 67, 836-843, 2022.

658 Cao, S., Cao, G., Chen, K., Han, G., Liu, Y., Yang, Y., and Li, X.: Characteristics of CO₂, water vapor,
659 and energy exchanges at a headwater wetland ecosystem of the Qinghai Lake, *Canadian Journal of Soil
660 Science*, 99, 227-243, [10.1139/cjss-2018-0104](https://doi.org/10.1139/cjss-2018-0104), 2019.

661 Carey, E. V., Sala, A., Keane, R., and Callaway, R. M.: Are old forests underestimated as global carbon
662 sinks?, *Global Change Biology*, 7, 339-344, [10.1046/j.1365-2486.2001.00418.x](https://doi.org/10.1046/j.1365-2486.2001.00418.x), 2001.

663 Chen, H., Ju, P. J., Zhu, Q., Xu, X. L., Wu, N., Gao, Y. H., Feng, X. J., Tian, J. Q., Niu, S. L., Zhang, Y.
664 J., Peng, C. H., and Wang, Y. F.: Carbon and nitrogen cycling on the Qinghai-Tibetan Plateau, *NATURE
665 REVIEWS EARTH & ENVIRONMENT*, 3, 701-716, [10.1038/s43017-022-00344-2](https://doi.org/10.1038/s43017-022-00344-2), 2022.

666 Cole, J. J., Caraco, N. F., Kling, G. W., and Kratz, T. K.: Carbon dioxide supersaturation in the surface
667 waters of lakes, *Science*, 265, 1568-1570, 1994.

668 Dass, P., Houlton, B. Z., Wang, Y., and Warlind, D.: Grasslands may be more reliable carbon sinks than
669 forests in California, *Environmental Research Letters*, 13, 074027, [10.1088/1748-9326/aacb39](https://doi.org/10.1088/1748-9326/aacb39), 2018.

670 Davidson, E. A., Richardson, A. D., Savage, K. E., and Hollinger, D. Y.: A distinct seasonal pattern of
671 the ratio of soil respiration to total ecosystem respiration in a spruce-dominated forest, *Global Change
672 Biology*, 12, 230-239, <https://doi.org/10.1111/j.1365-2486.2005.01062.x>, 2006.

673 Du, C., Zhou, G., and Gao, Y.: Grazing exclusion alters carbon flux of alpine meadow in the Tibetan
674 Plateau, *Agricultural and Forest Meteorology*, 314, 108774, 2022a.

675 Du, Y., Pei, W., Zhou, H., Li, J., Wang, Y., and Chen, K.: Net ecosystem exchange of carbon dioxide
676 fluxes and its driving mechanism in the forests on the Tibetan Plateau, *Biochemical Systematics and
677 Ecology*, 103, [10.1016/j.bse.2022.104451](https://doi.org/10.1016/j.bse.2022.104451), 2022b.

678 Ebermayer, E.: Die gesammte Lehre der Waldstreu mit Rücksicht auf die chemische Statik des

679 Waldbaues: unter Zugrundlegung der in den Königl. Staatsforsten Bayerns angestellten Untersuchungen,
680 Springer 1876.

681 Edwards, N. T.: Effects of Temperature and Moisture on Carbon Dioxide Evolution in a Mixed Deciduous
682 Forest Floor, Soil Science Society of America Journal, 39, 361-365,
683 <https://doi.org/10.2136/sssaj1975.03615995003900020034x>, 1975.

684 Falge, E., Baldocchi, D., Tenhunen, J., Aubinet, M., Bakwin, P., Berbigier, P., Bernhofer, C., Burba, G.,
685 Clement, R., Davis, K. J., Elbers, J. A., Goldstein, A. H., Grelle, A., Granier, A., Guðmundsson, J.,
686 Hollinger, D., Kowalski, A. S., Katul, G., Law, B. E., Malhi, Y., Meyers, T., Monson, R. K., Munger, J.
687 W., Oechel, W., Paw U, K. T., Pilegaard, K., Rannik, Ü., Rebmann, C., Suyker, A., Valentini, R., Wilson,
688 K., and Wofsy, S.: Seasonality of ecosystem respiration and gross primary production as derived from
689 FLUXNET measurements, Agricultural and Forest Meteorology, 113, 53-74,
690 [https://doi.org/10.1016/S0168-1923\(02\)00102-8](https://doi.org/10.1016/S0168-1923(02)00102-8), 2002.

691 Falge, E., Baldocchi, D., Olson, R., Anthoni, P., Aubinet, M., Bernhofer, C., Burba, G., Ceulemans, R.,
692 Clement, R., Dolman, H., Granier, A., Gross, P., Grünwald, T., Hollinger, D., Jensen, N.-O., Katul, G.,
693 Kerönen, P., Kowalski, A., Lai, C. T., Law, B. E., Meyers, T., Moncrieff, J., Moors, E., Munger, J. W.,
694 Pilegaard, K., Rannik, Ü., Rebmann, C., Suyker, A., Tenhunen, J., Tu, K., Verma, S., Vesala, T., Wilson,
695 K., and Wofsy, S.: Gap filling strategies for defensible annual sums of net ecosystem exchange,
696 Agricultural and Forest Meteorology, 107, 43-69, [https://doi.org/10.1016/S0168-1923\(00\)00225-2](https://doi.org/10.1016/S0168-1923(00)00225-2), 2001.

697 Foken, T., Gööckede, M., Mauder, M., Mahrt, L., Amiro, B., and Munger, W.: Post-Field Data Quality
698 Control, in: Handbook of Micrometeorology: A Guide for Surface Flux Measurement and Analysis,
699 edited by: Lee, X., Massman, W., and Law, B., Springer Netherlands, Dordrecht, 181-208, 10.1007/1-
700 4020-2265-4_9, 2005.

701 Hadden, D. and Grelle, A.: Net CO₂ emissions from a primary boreo-nemoral forest over a 10 year period,
702 Forest Ecology and Management, 398, 164-173, <https://doi.org/10.1016/j.foreco.2017.05.008>, 2017.

703 Hayek, M. N., Longo, M., Wu, J., Smith, M. N., Restrepo-Coupe, N., Tapajos, R., da Silva, R., Fitzjarrald,
704 D. R., Camargo, P. B., Hutryra, L. R., Alves, L. F., Daube, B., Munger, J. W., Wiedemann, K. T., Saleska,
705 S. R., and Wofsy, S. C.: Carbon exchange in an Amazon forest: from hours to years, Biogeosciences, 15,
706 4833-4848, 10.5194/bg-15-4833-2018, 2018.

707 Jia, X., Mu, Y., Zha, T., Wang, B., Qin, S., and Tian, Y.: Seasonal and interannual variations in ecosystem

708 respiration in relation to temperature, moisture, and productivity in a temperate semi-arid shrubland,
709 Science of The Total Environment, 709, 136210, <https://doi.org/10.1016/j.scitotenv.2019.136210>, 2020.

710 KATO, T., TANG, Y., GU, S., HIROTA, M., DU, M., LI, Y., and ZHAO, X.: Temperature and biomass
711 influences on interannual changes in CO₂ exchange in an alpine meadow on the Qinghai-Tibetan Plateau,
712 Global Change Biology, 12, 1285-1298, <https://doi.org/10.1111/j.1365-2486.2006.01153.x>, 2006.

713 Kondo, M., Saitoh, T. M., Sato, H., and Ichii, K.: Comprehensive synthesis of spatial variability in carbon
714 flux across monsoon Asian forests, Agricultural and Forest Meteorology, 232, 623-634, 2017.

715 Konopka, J., Heusinger, J., and Weber, S.: Extensive Urban Green Roof Shows Consistent Annual Net
716 Uptake of Carbon as Documented by 5 Years of Eddy-Covariance Flux Measurements, Journal of
717 Geophysical Research: Biogeosciences, 126, e2020JG005879, 2021.

718 Krasnova, A., Mander, Ü., Noe, S. M., Uri, V., Krasnov, D., and Soosaar, K.: Hemiboreal forests' CO₂
719 fluxes response to the European 2018 heatwave, Agricultural and Forest Meteorology, 323, 109042,
720 <https://doi.org/10.1016/j.agrformet.2022.109042>, 2022.

721 Landsberg, J. and Waring, R.: A generalised model of forest productivity using simplified concepts of
722 radiation-use efficiency, carbon balance and partitioning, Forest ecology and management, 95, 209-228,
723 1997.

724 Laurin, G. V., Chen, Q., Lindell, J. A., Coomes, D. A., Del Frate, F., Guerriero, L., Pirotti, F., and
725 Valentini, R.: Above ground biomass estimation in an African tropical forest with lidar and hyperspectral
726 data, ISPRS Journal of Photogrammetry and Remote Sensing, 89, 49-58, 2014.

727 Leuning, R. and King, K. M.: Comparison of eddy-covariance measurements of CO₂ fluxes by open-
728 and closed-path CO₂ analysers, Boundary-Layer Meteorology, 59, 297-311, 10.1007/BF00119818, 1992.

729 Li, L., Zhang, Y., Wu, J., Li, S., Zhang, B., Zu, J., Zhang, H., Ding, M., and Paudel, B.: Increasing
730 sensitivity of alpine grasslands to climate variability along an elevational gradient on the Qinghai-Tibet
731 Plateau, Science of the Total Environment, 678, 21-29, 2019.

732 Li, X. Y., Shi, F. Z., Ma, Y. J., Zhao, S. J., and Wei, J. Q.: Significant winter CO₂ uptake by saline lakes
733 on the Qinghai-Tibet Plateau, Global Change Biology, 28, 2041-2052, 2022.

734 Liu, C., Wu, Z., Hu, Z., Yin, N., Islam, A. T., and Wei, Z.: Characteristics and influencing factors of
735 carbon fluxes in winter wheat fields under elevated CO₂ concentration, Environmental Pollution, 307,
736 119480, 2022.

737 Liu, J., Zou, H.-X., Bachelot, B., Dong, T., Zhu, Z., Liao, Y., Plenković-Moraj, A., and Wu, Y.: Predicting
738 the responses of subalpine forest landscape dynamics to climate change on the eastern Tibetan Plateau,
739 *Global Change Biology*, 27, 4352-4366, <https://doi.org/10.1111/gcb.15727>, 2021.

740 Liu, N.-Y., Yang, Q.-Y., Wang, J.-H., Zhang, S.-B., Yang, Y.-J., and Huang, W.: Differential Effects of
741 Increasing Vapor Pressure Deficit on Photosynthesis at Steady State and Fluctuating Light, *Journal of*
742 *Plant Growth Regulation*, 10.1007/s00344-024-11268-0, 2024.

743 Lloyd, J. and Taylor, J. A.: On the temperature dependence of soil respiration, *Functional Ecology*, 8,
744 315-323, 1994.

745 Mamkin, V., Avilov, V., Ivanov, D., Varlagin, A., and Kurbatova, J.: Interannual variability in the
746 ecosystem CO₂ fluxes at a paludified spruce forest and ombrotrophic bog in the southern taiga,
747 *Atmospheric Chemistry and Physics*, 23, 2273-2291, 10.5194/acp-23-2273-2023, 2023.

748 Mao, D., Luo, L., Wang, Z., Zhang, C., and Ren, C.: Variations in net primary productivity and its
749 relationships with warming climate in the permafrost zone of the Tibetan Plateau, *Journal of*
750 *Geographical Sciences*, 25, 967-977, 10.1007/s11442-015-1213-8, 2015.

751 Mauder, M. and Foken, T.: Documentation and Instruction Manual of the Eddy-Covariance Software
752 Package TK3 (update),

753 Mizoguchi, Y., Ohtani, Y., Takanashi, S., Iwata, H., Yasuda, Y., and Nakai, Y.: Seasonal and interannual
754 variation in net ecosystem production of an evergreen needleleaf forest in Japan, *Journal of Forest*
755 *Research*, 17, 283-295, 10.1007/s10310-011-0307-0, 2012.

756 Moncrieff, J. B., Massheder, J. M., de Bruin, H., Elbers, J., Friborg, T., Heusinkveld, B., Kabat, P., Scott,
757 S., Soegaard, H., and Verhoef, A.: A system to measure surface fluxes of momentum, sensible heat, water
758 vapour and carbon dioxide, *Journal of Hydrology*, 188-189, 589-611, [https://doi.org/10.1016/S0022-](https://doi.org/10.1016/S0022-1694(96)03194-0)
759 [1694\(96\)03194-0](https://doi.org/10.1016/S0022-1694(96)03194-0), 1997.

760 Monson, R. K., Lipson, D. L., Burns, S. P., Turnipseed, A. A., Delany, A. C., Williams, M. W., and
761 Schmidt, S. K.: Winter forest soil respiration controlled by climate and microbial community
762 composition, *Nature*, 439, 711-714, 10.1038/nature04555, 2006.

763 Monteith, J. L., Unsworth, M. H., and Webb, A.: Principles of environmental physics, *Quarterly Journal*
764 *of the Royal Meteorological Society*, 120, 1699, 1994.

765 Mu, C., Mu, M., Wu, X., Jia, L., Fan, C., Peng, X., Ping, C. I., Wu, Q., Xiao, C., and Liu, J.: High carbon

766 emissions from thermokarst lakes and their determinants in the Tibet Plateau, *Global Change Biology*,
767 2023.

768 Niu, Z., Jinniu, W., Xufeng, W., Dongliang, L., Cheng, S., and Aihong, G.: Net ecosystem CO₂ exchange
769 and its influencing factors in non-growing season at a sub-alpine forest in the core Three Parallel Rivers
770 region, *Acta Ecologica Sinica*, 43, 5967-5979, 10.5846/stxb202204020841, 2023.

771 World Meteorological Organization.: 2019 concludes a decade of exceptional global heat and high-
772 impactweather[EB/OL].[https://public.wmo.int/en/media/press-release/2019-concludes-decade-of-](https://public.wmo.int/en/media/press-release/2019-concludes-decade-of-exceptional-global-heat-and-high-impact-weather)
773 [exceptional-global-heat-and-high-impact-weather](https://public.wmo.int/en/media/press-release/2019-concludes-decade-of-exceptional-global-heat-and-high-impact-weather), 2019.

774 Pan, Y., Birdsey, R. A., Fang, J., Houghton, R., Kauppi, P. E., Kurz, W. A., Phillips, O. L., Shvidenko, A.,
775 Lewis, S. L., and Canadell, J. G.: A large and persistent carbon sink in the world's forests, *Science*, 333,
776 988-993, 2011.

777 Pavelka, M., Acosta, M., Marek, M. V., Kutsch, W., and Janous, D.: Dependence of the Q₁₀ values on
778 the depth of the soil temperature measuring point, *Plant and Soil*, 292, 171-179, 10.1007/s11104-007-
779 9213-9, 2007.

780 Qu, S., Xu, R., Yu, J., and Borjigidai, A.: Extensive atmospheric methane consumption by alpine forests
781 on Tibetan Plateau, *Agricultural and Forest Meteorology*, 339, 109589,
782 <https://doi.org/10.1016/j.agrformet.2023.109589>, 2023.

783 Reichstein, M., Falge, E., Baldocchi, D., Papale, D., Aubinet, M., Berbigier, P., Bernhofer, C., Buchmann,
784 N., Gilmanov, T., Granier, A., Grünwald, T., Havránková, K., Ilvesniemi, H., Janous, D., Knohl, A.,
785 Laurila, T., Lohila, A., Loustau, D., Matteucci, G., Meyers, T., Miglietta, F., Ourcival, J.-M., Pumpanen,
786 J., Rambal, S., Rotenberg, E., Sanz, M., Tenhunen, J., Seufert, G., Vaccari, F., Vesala, T., Yakir, D., and
787 Valentini, R.: On the separation of net ecosystem exchange into assimilation and ecosystem respiration:
788 review and improved algorithm, *Global Change Biology*, 11, 1424-1439, [https://doi.org/10.1111/j.1365-](https://doi.org/10.1111/j.1365-2486.2005.001002.x)
789 [2486.2005.001002.x](https://doi.org/10.1111/j.1365-2486.2005.001002.x), 2005.

790 Schotanus, P., Nieuwstadt, F. T. M., and De Bruin, H. A. R.: Temperature measurement with a sonic
791 anemometer and its application to heat and moisture fluxes, *Boundary-Layer Meteorology*, 26, 81-93,
792 10.1007/BF00164332, 1983.

793 Schweizer, V. J., Ebi, K. L., van Vuuren, D. P., Jacoby, H. D., Riahi, K., Strefler, J., Takahashi, K., van
794 Ruijven, B. J., and Weyant, J. P.: Integrated Climate-Change Assessment Scenarios and Carbon Dioxide

795 Removal, *One Earth*, 3, 166-172, 10.1016/j.oneear.2020.08.001, 2020.

796 Schwinning, S. and Sala, O. E.: Hierarchy of responses to resource pulses in arid and semi-arid
797 ecosystems, *Oecologia*, 141, 211-220, 10.1007/s00442-004-1520-8, 2004.

798 Stein, T.: Carbon dioxide peaks near 420 parts per million at Mauna Loa observatory, NOAA Research,
799 June, 7, 2021.

800 Tang, X., Xiao, J., Ma, M., Yang, H., Li, X., Ding, Z., Yu, P., Zhang, Y., Wu, C., Huang, J., and Thompson,
801 J. R.: Satellite evidence for China's leading role in restoring vegetation productivity over global karst
802 ecosystems, *Forest Ecology and Management*, 507, 120000,
803 <https://doi.org/10.1016/j.foreco.2021.120000>, 2022.

804 Vote, C., Hall, A., and Charlton, P.: Carbon dioxide, water and energy fluxes of irrigated broad-acre crops
805 in an Australian semi-arid climate zone, *Environmental Earth Sciences*, 73, 449-465, 2015.

806 Wang, C.-Y., Wang, J.-N., Wang, X.-F., Luo, D.-L., Wei, Y.-Q., Cui, X., Wu, N., and Bagaria, P.:
807 Phenological Changes in Alpine Grasslands and Their Influencing Factors in Seasonally Frozen Ground
808 Regions Across the Three Parallel Rivers Region, Qinghai-Tibet Plateau, *Frontiers in Earth Science*, 9,
809 10.3389/feart.2021.797928, 2022.

810 Wang, S., Grant, R., Verseghy, D., and Black, T.: Modelling plant carbon and nitrogen dynamics of a
811 boreal aspen forest in CLASS—the Canadian Land Surface Scheme, *Ecological Modelling*, 142, 135-
812 154, 2001.

813 Wang, Y., Yao, G., Zuo, Y., and Wu, Q.: Implications of global carbon governance for corporate carbon
814 emissions reduction, *Frontiers in Environmental Science*, 11, 3, 2023a.

815 Wang, Y., Sun, Y., Chen, Y., Wu, C., Huang, C., Li, C., and Tang, X.: Non-linear correlations exist
816 between solar-induced chlorophyll fluorescence and canopy photosynthesis in a subtropical evergreen
817 forest in Southwest China, *Ecological Indicators*, 157, 111311,
818 <https://doi.org/10.1016/j.ecolind.2023.111311>, 2023b.

819 Wang, Y., Xiao, J., Ma, Y., Ding, J., Chen, X., Ding, Z., and Luo, Y.: Persistent and enhanced carbon
820 sequestration capacity of alpine grasslands on Earth's Third Pole, *Science Advances*, 9,
821 eade6875, doi:10.1126/sciadv.ade6875, 2023c.

822 Wang, Y., Xiao, J., Ma, Y., Luo, Y., Hu, Z., Li, F., Li, Y., Gu, L., Li, Z., and Yuan, L.: Carbon fluxes and
823 environmental controls across different alpine grassland types on the Tibetan Plateau, *Agricultural and*

824 Forest Meteorology, 311, 108694, 2021.

825 Wehr, R., Munger, J. W., McManus, J. B., Nelson, D. D., Zahniser, M. S., Davidson, E. A., Wofsy, S. C.,
826 and Saleska, S. R.: Seasonality of temperate forest photosynthesis and daytime respiration, *Nature*, 534,
827 680-683, 10.1038/nature17966, 2016.

828 Wu, T., Ma, W., Wu, X., Li, R., Qiao, Y., Li, X., Yue, G., Zhu, X., and Ni, J.: Weakening of carbon sink
829 on the Qinghai–Tibet Plateau, *Geoderma*, 412, 115707, <https://doi.org/10.1016/j.geoderma.2022.115707>,
830 2022.

831 Y, W. Z., Y, L. Z., K, D. S., L, F. M., S, L. Y., M, L. S., N, W. S., H, M. C., X, M. T., and Y, C.: Evolution
832 of ecological patterns and its driving factors on Qinghai-Tibet Plateau over the past 40 years, *Acta*
833 *Ecologica Sinica*, 42, 8941-8952, 2022.

834 Yasin, A., Niu, B., Chen, Z., Hu, Y., Yang, X., Li, Y., Zhang, G., Li, F., and Hou, W.: Effect of warming
835 on the carbon flux of the alpine wetland on the Qinghai-Tibet Plateau, *Frontiers in Earth Science*, 10,
836 10.3389/feart.2022.935641, 2022.

837 YU, G. and SUN, X.: Principles of flux measurement in terrestrial ecosystem, Beijing: Higher Education
838 Press, 2006.

839 Yu, Y.: Double-order system construction of China's climate change legislation under the dual carbon
840 goals, *China Population Resources and Environment*, 32, 89-96, 2022.

841 Zemin, Z., Fenggui, L., Qiong, C., Xingsheng, X., and Qiang, Z.: Spatial Prediction of Potential Property
842 Loss by Geological Hazards based on Random Forest—A Case Study of Chamdo, Tibet, *Plateau Science*
843 *Research*, 7, 21-30, 10.16249/j.cnki.2096-4617.2023.02.003, 2023.

844 Zhang, J., Lin, H., Li, S., Yang, E., Ding, Y., Bai, Y., and Zhou, Y.: Accurate gas extraction (AGE) under
845 the dual-carbon background: Green low-carbon development pathway and prospect, *Journal of Cleaner*
846 *Production*, 134372, 2022.

847 Zhang, Y., Zhu, W., Sun, X., and Hu, Z.: Carbon dioxide flux characteristics in an *Abies fabri* mature
848 forest on Gongga Mountain, Sichuan, China, *Acta Ecologica Sinica*, 38, 6125-6135, 2018.

849